EWSHM 2024
11th European Workshop on Structural Health Monitoring

Combined Passive and Active Ultrasonic Stress Wave Monitoring of Concrete Structures: An Overview of Data Analysis Techniques and Their Applications and Limitations

Thomas SCHUMACHER [1], Numa BERTOLA [2, 3], Niklas EPPLE [4],
Eugen BRUEHWILER [2], Ernst NIEDERLEITHINGER [4]
[1] Civil and Environmental Engineering, Portland State University Portland, OR, USA, thomas.schumacher@pdx.edu
[2] Ecole Polytechnique Fédérale de Lausanne (EPFL), Structural Engineering Institute, Lausanne, Switzerland, eugen.bruehwiler@epfl.ch
[3] University of Luxembourg, Department of Engineering, Esch-sur-Alzette, Luxembourg, numa.bertola@uni.lu
[4] Bundesanstalt für Materialforschung und -prüfung, Berlin, Germany, niklas.epple@bam.de, ernst.niederleithinger@bam.de

Abstract. Combined passive ultrasonic (US) stress wave [better known as acoustic emission (AE)] and active US stress wave monitoring has been shown to provide a more holistic picture of ongoing fracture processes, damage progression, as well as slowly occurring aging and degradation mechanisms in concrete structures. Traditionally, different data analysis techniques have been used to analyze the data generated from these two monitoring techniques. For passive US stress wave monitoring, waveform amplitudes, hit rates, source localization, and *b*-value analysis, among others, have been used to detect and locate cracking. On the other hand, amplitude tracking, magnitude squared coherence (MSC), and coda wave interferometry (CWI) are examples of analyses that have been employed for active US stress wave monitoring. In this paper, we explore some of these data analysis techniques and show where their respective applications and limitations might be. After providing an overview of the monitoring approach and the different data analysis techniques, results and observations from selected laboratory experiments are discussed. Finally, suggestions for further work are proposed.

Keywords: Combined passive and active ultrasonic stress wave monitoring; Structural health monitoring; Concrete structures; Asset management.

Media and Publishing Partner
https://doi.org/10.58286/29863

Introduction

The integration of passive ultrasonic (US) stress wave [better known as acoustic emission (AE)] and active US stress wave monitoring have shown to improve capabilities with respect to capturing ongoing fracture processes as well as slowly-varying degradation processes in large-scale and real concrete structures [1, 2]. This combined approach is based on the same underlying physics (i.e., wave motion in solids) and can be implemented using the same instrumentation, i.e., US transducers and data acquisition system. To ensure that the transducer coupling remains constant over time, embedded US transducers have been evaluated [3-5] and were used herein. While the two monitoring techniques have traditionally employed their own data analysis techniques, it can be argued that some of them could be useful for both, and selection depends on what internal changes should be monitored and the level of sensitivity deemed necessary. This paper explores some of the common analysis techniques and demonstrates their applications and limitations.

1. Analysis Techniques

Common analyses used for passive US stress wave (or AE) monitoring include parameter-based and signal-based techniques [6-8]. The latter can be further sub-divided into waveform and quantitative analyses. While parameter and waveform analyses can be performed with the measurements from a single transducer (i.e., they are considered hit-based), quantitative analyses require measurements from multiple transducers (i.e., they are referred to as event-based). Active US stress wave monitoring has been performed in the past by simple time of flight/velocity measurements. Recent research is focused on coda wave analysis, mainly using coda-wave interferometry (CWI) which is much more sensitive. Table 1 lists the selected analysis techniques explored in this paper. Note that passive US stress wave monitoring is, by definition, on-demand, and records data based on the level of activity given at any time. On the other hand, active US stress wave monitoring is typically initiated based on a predefined schedule. If desired, the pulse repetition frequency (PRF) can be set to a value sufficiently small to capture transient loadings such as a passing truck.

Table 1. Overview of analysis techniques explored in this paper. Selected from [6-9].

Analysis technique	Passive US stress wave (or AE) monitoring	Active US stress wave monitoring	Example Section 2
Hit rates vs. time	Level of activity	Not used	1
Hit (or waveform) amplitude, A vs. time	Strength of released energy	Level of applied load and amount of distress (low sensitivity)	1
Coda wave interferometry (CWI) applied to two waveforms: Stretch factor, $\varepsilon = dv/v$ and cross-correlation coefficient, CC (between two waveforms)	Not used	Level of applied load, micro-cracking, slowly varying deterioration processes, and temperature (high sensitivity)	1, 3
Event rates vs. time	Not used	Presence of distress	2
Source localization	Regions with active fracture processes	Regions of distress (based on location error)	2

2. Examples

In this section, results from two laboratory experiments and ongoing monitoring of an in-service bridge using US stress wave-based monitoring are presented. These were selected to demonstrate the applications and limitations of the analysis techniques listed in Table 1.

2.1 Example 1: Laboratory Testing of a Full-Scale Reinforced Concrete Bridge Column

In this example, results from a laboratory experiment on a full-scale column-footing subassembly representative of an existing bridge bent are presented. The loading protocol, which includes cyclic lateral loading and varying axial loading, is shown in Fig. 1 (a). The goal of the research was to determine the seismic performance of a typical reinforced concrete bridge in Oregon having pre-1990s reinforcement detailing in the plastic hinge region [10]. Fig. 1 (b) illustrates the observed damage states (DS) throughout the test. The numbered labels in Fig. 1 (a) refer to specific performance changes and are described in detail in [11]. Fig. 1 (b) shows an elevation view of the test specimen with embedded reinforcement. Instrumentation relevant to this study includes five US transducers, of which three surface-mounted (AE1 through AE3) and three were embedded in the concrete (US1, US2, UST). The former and latter were used for passive US stress wave (or AE) and active US stress wave monitoring. AE data were collected trigger-based for hits with a waveform amplitude, $A > 35$ dB. The US transducer labeled UST was used to transmit a 60 kHz Morlet-type pulse every 1 s throughout the experiment, forming two US regions labeled R1 and R2. Additional details regarding the US transducers and data acquisition system used can be found in [11].

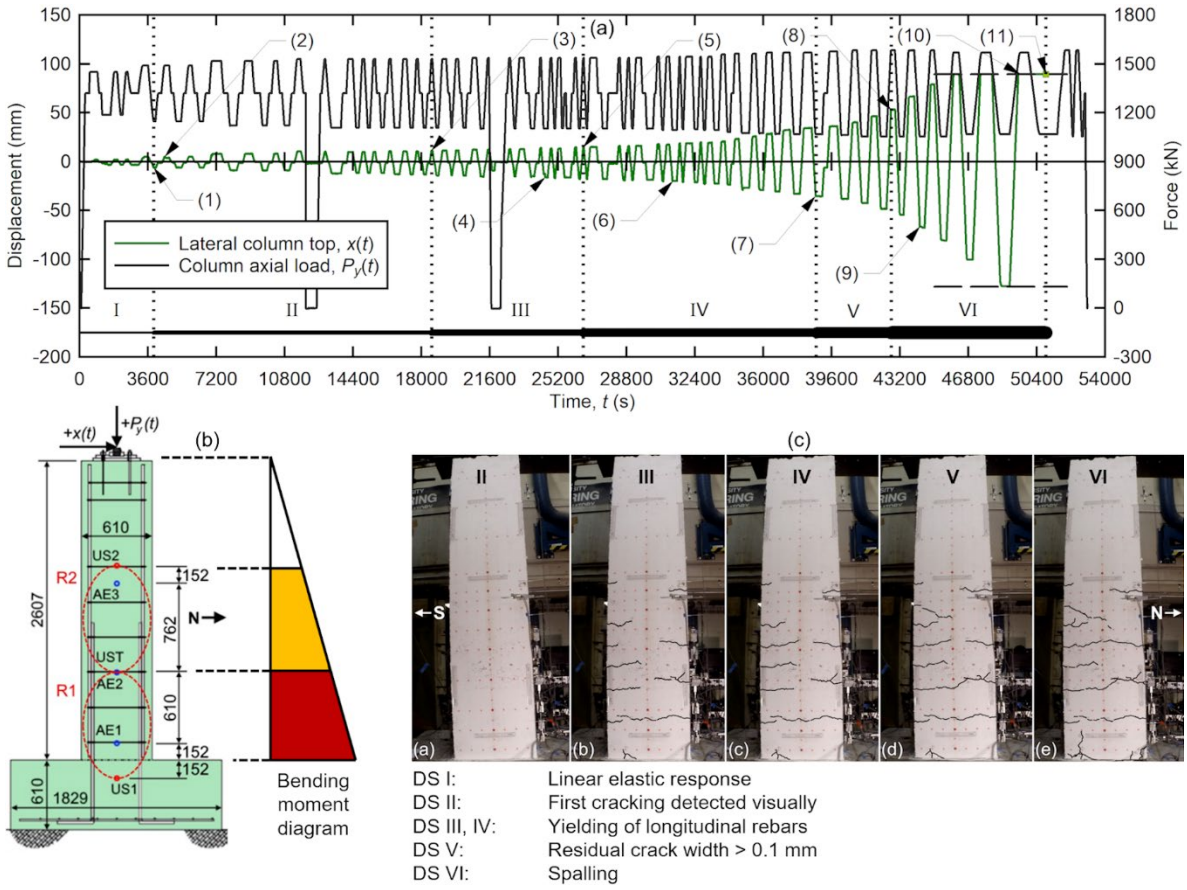

Fig. 1. (a) Loading protocol (entire experiment) showing applied column top lateral displacement, $x(t)$ (left y-axis) and column axial load, $P_y(t)$ (right y-axis) vs. time, (b) elevation view of test specimen with instrumentation and bending moment diagram, and (b) photos of column corresponding to DS II through VI. All dimensions in (c) in mm.

Fig. 2 provides an overview of sample analysis results for DS I and II (see Table 1 for the analysis techniques selected for this example). These two damage states were selected because they contain the transition from a linearly elastic (DS I) to an inelastic (DS II) response of the test specimen. The passive US stress wave (or AE) response at transducer AE 1 is shown in (b). Note that while the amplitude plots were visually very similar among transducers AE1 through AE 3, the cumulative number of AE hits decreased notably with increasing column height. This can be explained by the lower bending moment demand with increasing column height [see bending moment diagram in (b)], which corresponds to fewer cracks and cracks with smaller width [see (c)]. Fig. 2 (c) through (e) and (f) through (h) show the active US stress wave monitoring results pertaining to US regions R2 and R1, respectively.

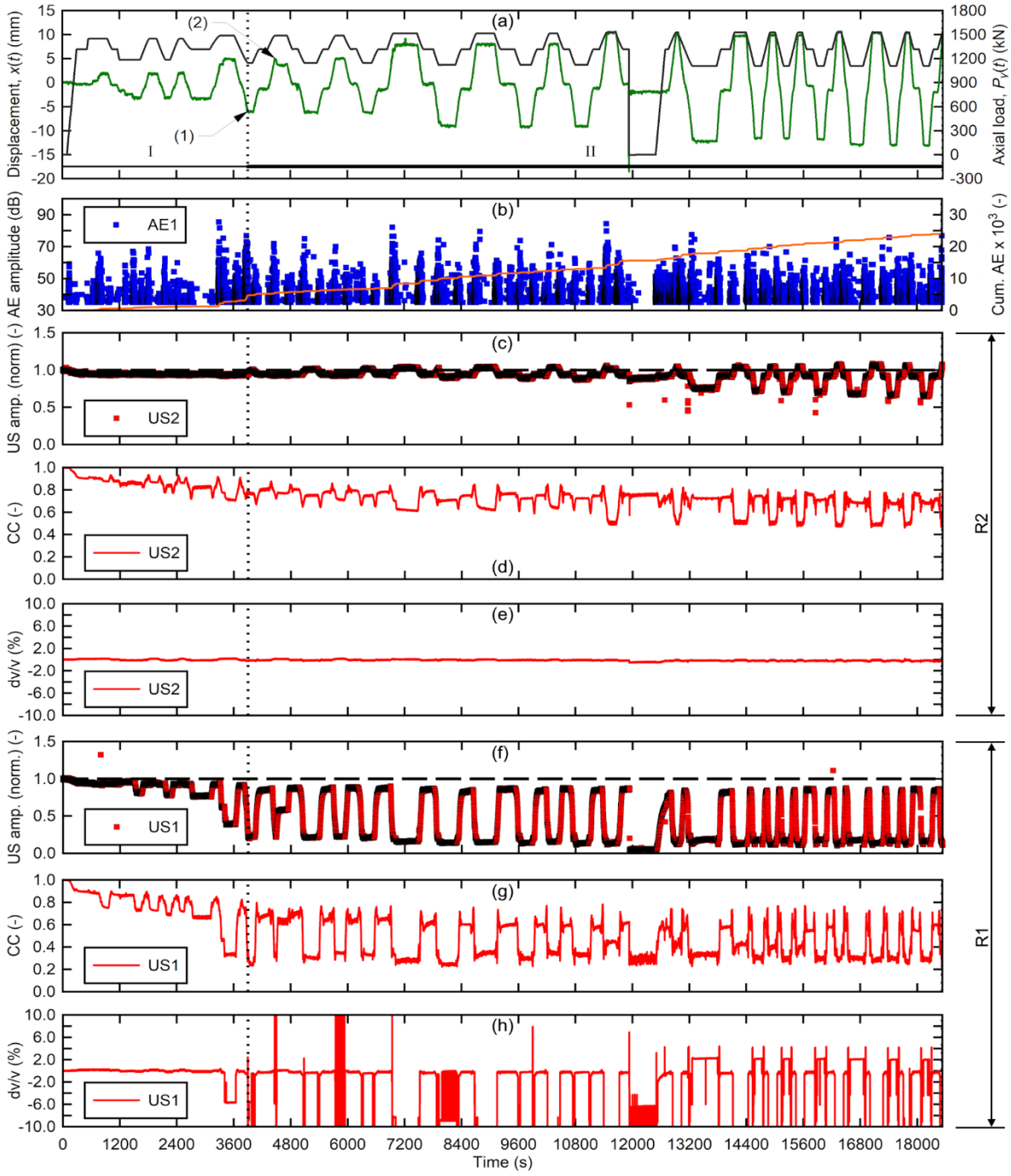

Fig. 2. (a) Loading protocol (DS I and II) showing applied column top lateral displacement, $x(t)$ (left y-axis) and column axial load, $P_y(t)$ (right y-axis) vs. time, (b) AE waveform amplitudes and cumulative AE hits (x 1000) vs. time for AE1, (c) through (e) US results for R1 vs. time, and (f) through (h) US results for R2 vs. time.

Overall, all three US variables, i.e., US waveform amplitude, A, cross-correlation coefficient, CC, and coda wave stretch factor, $\varepsilon = dv/v$ exhibit larger variations vs. time for R1 compared to R2. This is consistent with the AE response shown in (b). It can further be observed that CC and A have similar trends with the former being more sensitive; ε is technically only applicable in a continuum, since it assumes a slight stretch between two waveforms that are otherwise similar. The implication of this is that ε is not valid after cracks form, which can be seen by the strong variation of this variable in DS II.

2.2 Example 2: Laboratory Testing of a Large-Scale UHPFRC T-beam

In this example, selected analysis results are presented from a research project conducted to evaluate the use of combined US stress wave monitoring on an ultra-high performance fiber-reinforced cementitious composite (UHPFRC) T-beam during experimental load testing (Phase 2). Results from the early-age monitoring phase (Phase 1) are discussed in [12]. Fig. 3 shows the experimental test setup, specimen, and instrumentation.

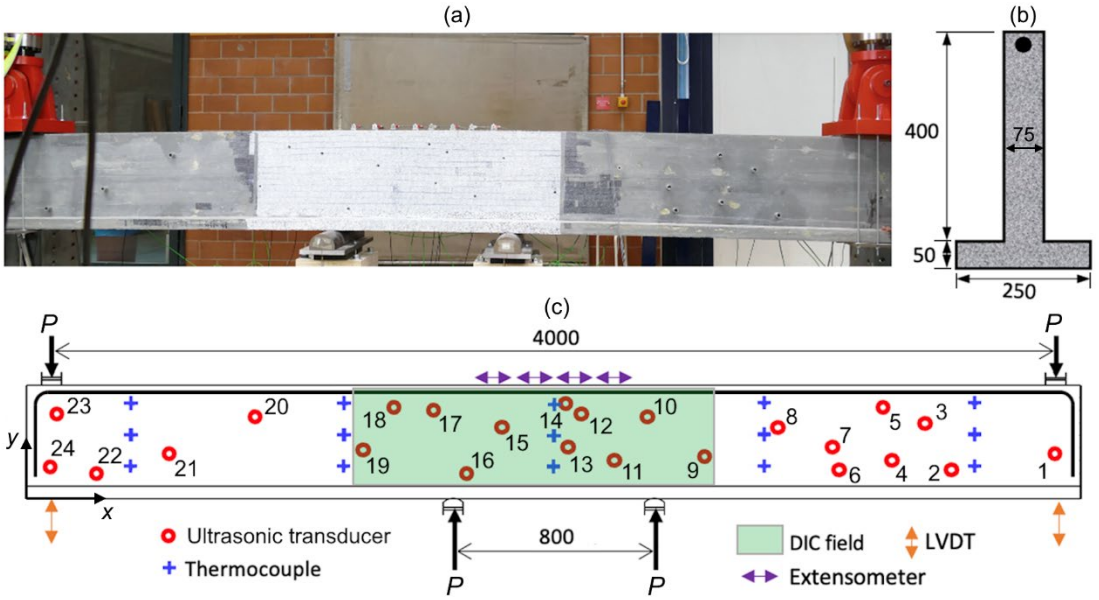

Fig. 3. Experimental test setup and specimen: (a) Photo of test specimen, (b) cross-section of test specimen, and (c) elevation view of test specimen with instrumentation. All dimensions in mm.

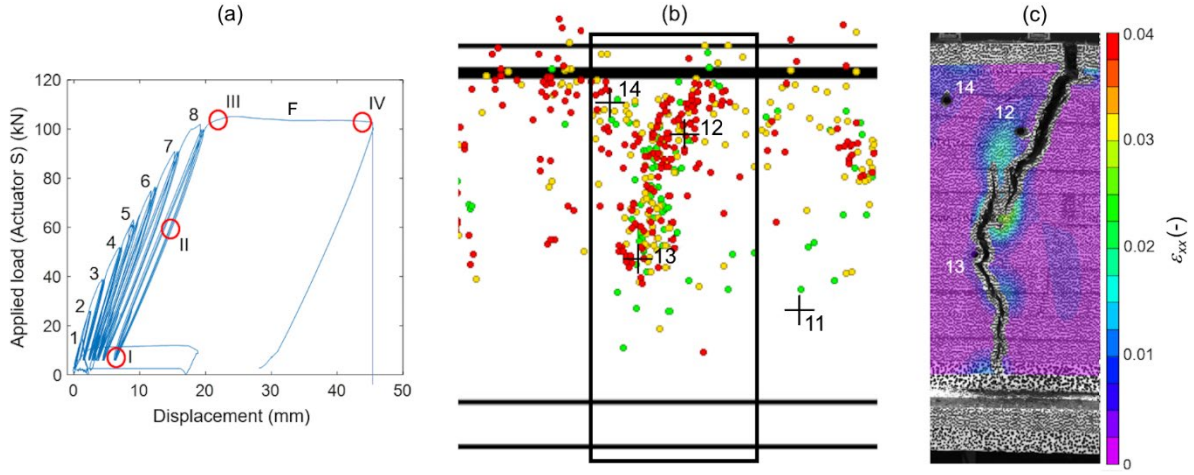

Fig. 4. (a) Load, P vs. beam displacement (entire Phase 2). LCG are numbered 1 through F (F = final loading leading to failure), (b) Located AE events for LCG 2 (all load cycles), (c) DIC-computed strain field for point "IV" on final load cycle "F". Green, yellow, and red dots in (b) correspond to location uncertainties (LUCY) for LUCY ≤ 10 mm, 10 mm < LUCY ≤ 25 mm, and 25 mm < LUCY ≤ 50 mm, respectively.

In Fig. 4 (a), the loading protocol is illustrated with numbers indicating the load cycle group (LCG); (b) shows located AE events for LCG 2 and (c) shows the surface strain field computed using digital image correlation (DIC). It can be observed that during LCG 2, the failure crack, while not detectable visually during this LCG, matches with the cluster of located AE events. Fig. 5 shows the distributions of AE sources along the specimen's *x*-location for LCG 1 through 8, corresponding to (b) through (i), respectively. It can be observed that the bins closest to the location of the failure crack show the highest number of cumulative located events. The ability to predict the potential failure location of structural members made of UHPFRC is useful since these members develop fewer cracks and at a later stage in the loading process compared to conventional RC members.

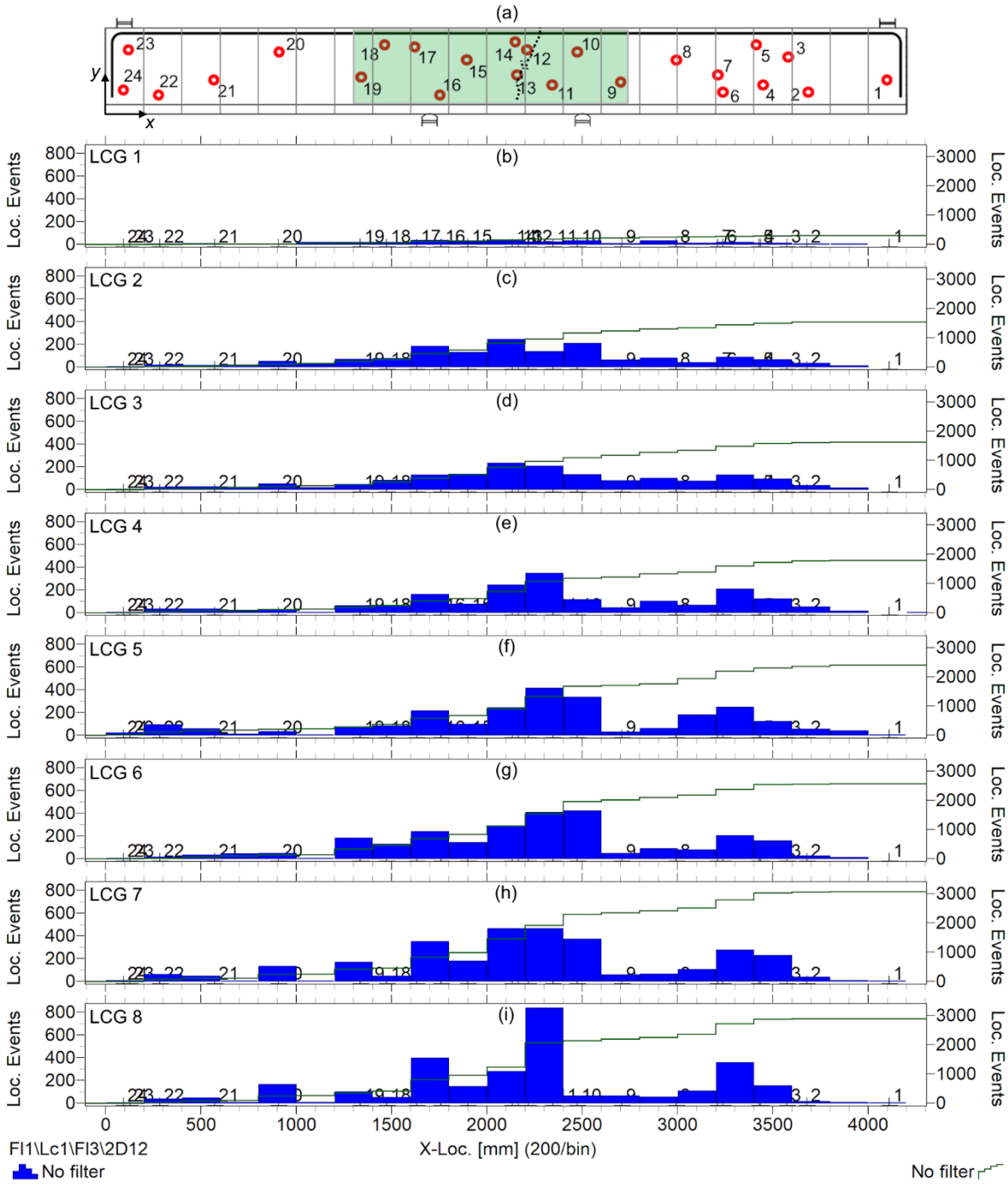

Fig. 5. (a) Elevation view of test specimen with US transducers, (b) through (i) distribution of located AE events (left *y*-axis) and cumulative located AE events (right *y*-axis) vs. *x*-location for LCG 1 through 8. The vertical grey lines in (a) delineate the bins (width = 200 mm) used in (b) through (i).

2.3 Example 3: Monitoring of Full-scale Bridge Girders

Several two-span post-tensioned girders were subjected to load tests as part of a research project organized and funded by the Federal Highway Research Institute (BASt) of Germany [16]. Objectives were to check current codes, which are based on the result of single-span experiments only and to understand details of stress and strain distributions as well as failure mechanism for certain geometries [17]. One of the girders, which has an H-shaped cross-section, is shown in Fig. 6. Loading was provided by two point loads applied slightly off-center on each span. The experiments were monitored by various conventional sensors and DIC [20]. In addition, a section of the beam was equipped with 20 embedded US transducers, the same type as in the experiment described in Sections 2.1 and 2.2.

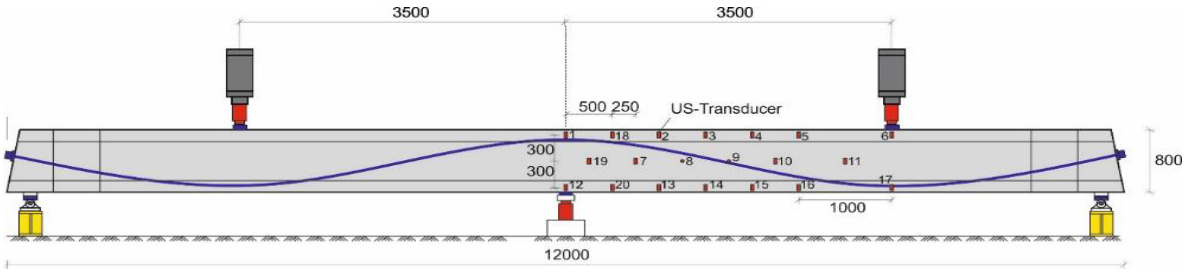

Fig. 6. Sketch of load test setup for girder DLT 1.3 (dimensions in mm). Blue line: Tendon duct. Source: [18].

The strength of active US stress wave monitoring evaluated by CWI is its ability to detect changes and stresses in an early state (before visual damage). Fig 7 shows the distribution of US velocity changes in the instrumented part of the girder (simple interpolation of values calculated for each transducer pair, allocated to the center of each combination) at about 20% of the failure load. Strong velocity drops (yellow) appear on the opposite site of the loading/support points, caused by the tension and opening of microcracks there.

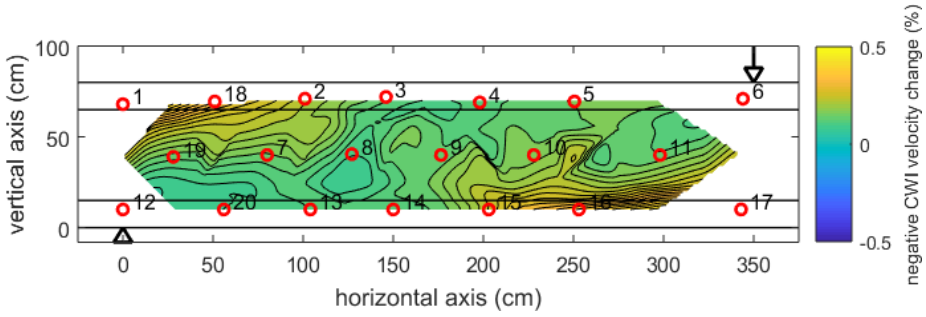

Fig. 7. US velocity change distribution at 250 kN load. From [18].

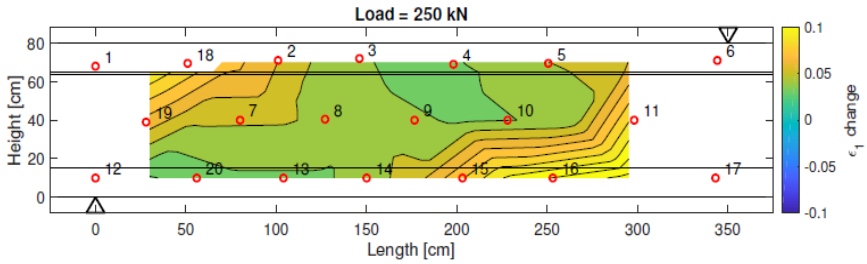

Fig. 8. Horizontal component of strain change at 250 kN load, determined from velocity changes. From [19].

Velocity changes cannot be used directly for structural assessment. To translate this parameter to something more useful, local calibration has to be performed. This was done by correlating velocity changes at one of the transducer pairs with the horizontally oriented strain gauge in the center of this pair [19]. The result is shown in Fig. 8 and can be used to validate engineering or numerical models.

3. Conclusions and Outlook

Combining passive and active US stress wave monitoring has been shown to provide a more holistic picture of ongoing fracture processes as well as slowly-varying degradation processes in concrete structures. This paper highlights different data analysis techniques and their applications and limitations. Specifically, CWI can track minute internal changes that can be related to engineering variables such as strain. Simple waveform parameters such as amplitude can be used when CWI fails due to its sensitivity to track the progression of cracking. Locating passive US stress wave (or AE) sources and visualizing their distributions can provide real-time information about the potential failure location. By selecting appropriate analyses, the two monitoring techniques can be integrated, allowing to take full advantage of their strengths. Future work is directed at understanding and accounting for environmental factors such as temperature, humidity, and transducer coupling.

References

[1] T. Schumacher and E. Niederleithinger, "Combining Passive and Active Ultrasonic Stress Wave Monitoring Techniques: Opportunities for Condition Evaluation of Concrete Structures," presented at the International Symposium on Non-Destructive Testing in Civil Engineering (NDT-CE 2022), Zurich, Switzerland, 2022.

[2] E. Niederleithinger, X. Wang, N. Epple, T. Schumacher, S. Ahmed, and P. Klikowicz, "Ultrasonic Coda Wave Monitoring of Concrete Structures: First Experiences with Large-scale Experiments and Real Structures," presented at the Tenth International Conference on Bridge Maintenance, Safety and Management (IABMAS 2020), Sapporo, Japan, 2021.

[3] E. Niederleithinger, J. Wolf, F. Mielentz, H. Wiggenhauser, and S. Pirskawetz, "Embedded Ultrasonic Transducers for Active and Passive Concrete Monitoring," *Sensors,* vol. 15, 2015.

[4] X. Wang, E. Niederleithinger, and I. Hindersmann, "The installation of embedded ultrasonic transducers inside a bridge to monitor temperature and load influence using coda wave interferometry technique," *Structural Health Monitoring,* vol. 21, pp. 913-927, 2021.

[5] A. Deraemaeker and C. Dumoulin, "Embedding ultrasonic transducers in concrete: A lifelong monitoring technology," *Construction and Building Materials,* vol. 194, pp. 42-50, 2019.

[6] T. Schumacher, L. M. Linzer, and C. Grosse, "Signal-based AE Analysis," in *Acoustic Emission Testing*, C. Grosse, M. Ohtsu, D. G. Aggelis, and T. Shiotani, Eds., Second ed Cham: Springer, 2022, pp. 73-116.

[7] T. Schumacher, B. Schechinger, and T. Vogel, "AE Monitoring of Real Structures: Applications, Strengths, and Limitations," in *Acoustic Emission Testing*, C. Grosse, M. Ohtsu, D. G. Aggelis, and T. Shiotani, Eds., Second ed Cham: Springer, 2022, pp. 731-752.

[8] D. G. Aggelis and T. Shiotani, "Parameters Based AE Analysis," in *Acoustic Emission Testing*, C. Grosse, M. Ohtsu, D. G. Aggelis, and T. Shiotani, Eds., Second ed Cham: Springer, 2022, pp. 45-71.

[9] J. H. Kurz, T. Schumacher, L. M. Linzer, B. Schechinger, and C. Grosse, "Source Localization," in *Acoustic Emission Testing*, C. Grosse, M. Ohtsu, D. G. Aggelis, and T. Shiotani, Eds., Second ed Cham: Springer, 2022, pp. 117-171.

[10] A. K. M. Murtuz, P. Dusicka, and T. Schumacher, "Seismic Performance Design Criteria for Bridge Bent Plastic Hinge Regions," Oregon Department of Transportation (ODOT), Samem, OR2020.

[11] T. Schumacher, M. Golam AKM, A. Hafiz, P. Dusicka, and E. Niederleithinger, "Post-Earthquake Damage Assessment of Reinforced Concrete Members using Combined Passive and Active Ultrasonic Stress Wave Monitoring," presented at the EWSHM, Palermo, Italy, 2022.

[12] N. Bertola, T. Schumacher, E. Niederleithinger, and E. Bruehwiler, "Combined Passive and Active Ultrasonic Stress Wave Monitoring of UHPFRC Properties on a Structural Level," presented at the International Interactive Symposium on Ultra-High Performance Concrete, Wilmington, DE, USA, 2023.

[16] E. Niederleithinger, X. Wang, M. Herbrand, M. Mueller. „Processing Ultrasonic Data by Coda Wave Interferometry to Monitor Load Tests of Concrete Beams“. *SENSORS* 18, Nr. 6 (Juni 2018). https://doi.org/10.3390/s18061971.

[17] J. Hegger, M. Herbrand, M. Maurer, K. Zilch, G.A. Rombach, Beurteilung der Querkraft und der Torsionstragfähigkeit von Brücken im Bestand—Erweiterte Bemessungsansätze; BASt Joint Research Project FE 15.0591/2012/FRB, Interim Report; RWTH University: Aachen, Germany, 2016.

[18] Herbrand, M.; Classen, M.; Adam, V. Querkraftversuche an Durchlaufträgern aus Spannbeton mit Rechteck- und I-Querschnitt. Bauingenieur 2017, 92, 465–473.

[19] N. Epple, From Seismology to Bridge Monitoring, Master thesis BAM/RWTH/ETH/TU Delft, 2018, http://resolver.tudelft.nl/uuid:9a8757f9-b282-47bc-bd06-8b9f6071c3d5